MOLECULAR AND CELLULAR BIOLOGY, May 2002, p. 2906–2917 Vol. 22, No. 9
0270-7306/02/$04.00+0 DOI: 10.1128/MCB.22.9.2906–2917.2002

DNA Methyltransferase Deficiency Modifies Cancer Susceptibility in Mice Lacking DNA Mismatch Repair

Binh N. Trinh,[1] Tiffany I. Long,[1] Andrea E. Nickel,[1] Darryl Shibata,[1,2] and Peter W. Laird[1,3]*

Department of Biochemistry and Molecular Biology,[1] Department of Pathology,[2] and Department of Surgery,[3] Norris Comprehensive Cancer Center, Keck School of Medicine, University of Southern California, Los Angeles, California 90089-9176

Received 30 October 2001/Returned for modification 14 January 2002/Accepted 29 January 2002

We have introduced DNA methyltransferase 1 (*Dnmt1*) mutations into a mouse strain deficient for the Mlh1 protein to study the interaction between DNA mismatch repair deficiency and DNA methylation. Mice harboring hypomorphic *Dnmt1* mutations showed diminished RNA expression and DNA hypomethylation but developed normally and were tumor free. When crossed to *Mlh1*$^{-/-}$ homozygosity, they were less likely to develop the intestinal cancers that normally arise in this tumor-predisposed, mismatch repair-deficient background. However, these same mice developed invasive T- and B-cell lymphomas earlier and at a much higher frequency than their *Dnmt1* wild-type littermates. Thus, the reduction of Dnmt1 activity has significant but opposing outcomes in the development of two different tumor types. DNA hypomethylation and mismatch repair deficiency interact to exacerbate lymphomagenesis, while hypomethylation protects against intestinal tumors. The increased lymphomagenesis in *Dnmt1* hypomorphic, *Mlh1*$^{-/-}$ mice may be due to a combination of several mechanisms, including elevated mutation rates, increased expression of proviral sequences or proto-oncogenes, and/or enhanced genomic instability. We show that CpG island hypermethylation occurs in the normal intestinal mucosa, is increased in intestinal tumors in *Mlh1*$^{-/-}$ mice, and is reduced in the normal mucosa and tumors of *Dnmt1* mutant mice, consistent with a role for Dnmt1-mediated CpG island hypermethylation in intestinal tumorigenesis.

Cancer development is thought be driven by the acquisition of both mutations and abnormal methylation patterns (4, 38). Aberrant hypermethylation of promoter CpG islands can lead to transcriptional silencing of key growth-controlling genes (4, 32, 38, 71). DNA methylation is also thought to play a role in the silencing of endogenous repetitive DNA elements such as transposons, retroviruses, LINE-1, and Alu sequences (30, 31, 42, 53, 82). The mechanism driving these methylation events is unclear, but it involves one or more of the DNA methyltransferase enzymes known to methylate genomic DNA at CpG sites.

DNA methyltransferase 1 (Dnmt1), Dnmt3a, and Dnmt3b are three functional DNA methyltransferase enzymes known to contribute to methylation patterns in mammalian cells. These enzymes have differential abilities to catalyze maintenance and de novo methylation (61). In vitro methylation studies have shown that while Dnmt1 has a strong predilection for hemimethylated DNA, Dnmt3a and Dnmt3b have approximately equivalent preferences for hemimethylated and unmethylated DNA substrates (61). This has led to the widely held concept that Dnmt1 is predominantly responsible for maintenance methylation, while Dnmt3a and Dnmt3b are primarily involved in de novo methylation. Some expression studies have suggested that abnormal upregulation of DNA methyltransferase genes might cause aberrant methylation patterns and thus enhance cancer risk, but others have argued against this mechanism (17, 24, 35, 40, 48, 69). The normal activity of methyltransferases may be dependent upon their proper interaction with PCNA through a conserved PCNA-binding motif (11, 83, 84), localization to replication foci during S phase (51), and cell cycle regulation (70). Deregulation of these activities may lead to irregular methylation patterns.

In this study we used a mouse model system to assess the interaction between DNA methylation and DNA mismatch repair deficiency. Cells lacking functional mismatch repair are subjected to 100- to 1,000-fold increases in microsatellite instability (MSI$^+$) and base substitution rates throughout the genome due to the inability to repair replication errors that create base-base and loop mismatched heteroduplex DNA (74). Targeted mutations have been generated for mismatch repair genes *Msh2*, *Msh3*, *Msh5*, *Msh6*, *Mlh1*, *Pms1*, and *Pms2* in mice (3, 15, 20, 21, 23, 64, 66). Mutant mice are prone to the development of a spectrum of tumors, in addition to a meiotic defect resulting in infertility (2, 3, 14, 20, 21). However, the mutation spectrum, tumor phenotype, and meiotic phenotype are not always manifest, nor are they the same in all mismatch repair mutant animals, indicating that these genes have distinct yet overlapping functions. Loss-of-function mutations in genes *MLH1*, *MSH2*, and *MSH6* are the most commonly observed mismatch repair gene mutations in colorectal cancer patients, suggesting that disruption of early steps in the DNA mismatch repair process causes a predisposition to colorectal tumorigenesis.

A role for DNA methylation in the mismatch repair pathway has been proposed (5, 29), possibly involving an interaction between DNA methyltransferase and PCNA (11, 68) and/or the assistance of methylation patterns in mismatch recognition and correction through MBD4 recruitment (5), but direct evidence in support of these mechanisms is lacking. In *Escherichia coli*, Dam methylation at GATC sites serves as the strand discrimination for the incision and excision of the DNA strand

* Corresponding author. Mailing address: Norris Comprehensive Cancer Center, 1441 Eastlake Ave., Los Angeles, CA 90089-9176. Phone: (323) 865-0650. Fax: (323) 865-0158. E-mail: plaird@hsc.usc.edu.

containing the mismatched base (54). However, model organisms such as *Saccharomyces cerevisiae* and *Caenorhabditis elegans* have functional mismatch repair despite having no detectable DNA methylation. It is speculated that the orientation of the passing replication fork complex and/or the presence of transient DNA nicks after replication may act as strand discrimination signals in these organisms (77, 78). Whether CpG hemimethylation participates as a signal for strand discrimination in mammalian cells has not been resolved.

Abnormal methylation patterns have been well documented in colorectal cancer (25, 27, 75, 86). Hypermethylation of the *MLH1* promoter has been shown to be the basis for the inactivation of the *MLH1* mismatch repair gene in the majority of the 10 to 15% of sporadic colorectal cancer cases that exhibit an MSI$^+$ phenotype (33, 81). Several studies have reported that mismatch repair deficiency is associated with a generalized CpG island methylation phenotype (1, 75). It has also been reported that MSI$^+$ colorectal cell lines have a higher de novo methylation activity towards exogenous retroviral sequences than those that are MSI$^-$ (50). However, we did not find an increased frequency of CpG island hypermethylation in MSI$^+$ colorectal cell lines (63) or colorectal tumors (86). We have recently suggested that the association between CpG island hypermethylation and mismatch repair deficiency is limited to the association with *MLH1* promoter hypermethylation (86). It has been reported that patients with MSI$^+$ cases show loss of imprinting of *IGF2* (13, 56). The significance of this observation is poorly understood, but it suggests that DNA methylation and mismatch repair pathways may be intertwined.

In this study, we have devised a genetic strategy based on *Dnmt1* hypomorphic alleles to study the effect of DNA methylation on tumor development (45). This system avoids the toxicity associated with the use of 5-aza-2′-deoxycytidine (37). Here, we made use of two hypomorphic alleles which, when introduced in combination, allow for manipulation of the levels of expression of Dnmt1 in vivo without compromising development (52). We applied this experimental system to a mouse *Mlh1* knockout strain that is predisposed to the development of multiple tumors, including lymphomas and intestinal adenocarcinomas (3). We show that hypomorphic alleles of *Dnmt1* can lead to decreased RNA expression, hypomethylation of centromeric repeat sequences, and reduced hypermethylation of promoter regions containing CpG islands. Paradoxically, a reduction in Dnmt1 expression concomitantly reduced the incidence of intestinal cancers and increased the incidence of aggressive lymphoid tumors in mismatch repair-deficient mice. Our data suggest that in the intestinal epithelium, Dnmt1 may contribute to cancer by causing CpG island hypermethylation. Further, we suggest that the mechanism by which lymphomagenesis is induced by DNA hypomethylation is distinct and possibly could involve a combination of molecular defects, including the lack of mismatch repair, a global change in gene expression patterns with upregulation of repetitive retroelements, and an increased chromosomal instability as a result of a hypomethylated genome.

MATERIALS AND METHODS

Genotyping. We used PCR to genotype the *Mlh1* gene as described previously by Baker et al. (3). The PCR was performed in a 15-μl reaction mixture with 20 mM Tris-HCl (pH 8.4); 50 mM KCl; 1.5 mM $MgCl_2$; 0.2 mM deoxynucleoside triphosphates; 0.3 μM primers MLH1-a, MLH1-U, and MLH1-T5; and 0.35 U of *Taq* polymerase, using cycling conditions of 94°C for 4 min, followed by 35 cycles of 94°C for 50 s, 58°C for 50 s, and 72°C for 60 s, followed by 72°C for 5 min. The MLH1-a and MLH1-U primers produced a 258-bp amplicon, while the MLH1-a and MLH1-T5 primers produced a 198-bp amplicon, which were diagnostic for the wild-type and targeted alleles, respectively.

Dnmt1 was genotyped by multiplex PCR using primers OL106 (5′-GGGAACTTCCTGACTAGGGG-3′), OL168, (5′CCAACAAACCAGTATGTCTCGT-3′), OL173 (5′-CCCAGTTTCCAGAAAGCTACC-3′), and OL369 (5′-CAATTCCACACAACATACGAGC-3′). Reactions were carried out in a 15-μl volume with 20 mM Tris-HCl (pH 8.4), 50 mM KCl, 1.5 mM $MgCl_2$, 0.2 mM deoxynucleoside triphosphates, a 0.3 μM concentration of each primer, and 0.35 U of *Taq* polymerase, using cycling conditions of 94°C for 4 min, followed by 35 cycles of 94°C for 50 s, 60°C for 50 s, and 72°C for 1 min 30 s, followed by 72°C for 5 min. OL168 and OL173 produced both a 342-bp wild-type-specific band and a 661-bp *Dnmt1*^{R} allele-specific band. OL106 and OL173 produced a 430-bp *Dnmt1*^{N} allele-specific band. OL173 and OL369 produced a second 211-bp *Dnmt1*^{R} allele-specific band.

Examination of mice. These experiments were conducted with F_1 mice derived from two inbred strains. All of the alleles used in this study had been backcrossed to 129/svJae or C57BL/6 mice for at least 10 generations before the experimental crosses were set up. We limited our analysis to homozygous *Mlh1*$^{-/-}$ and *Mlh1*$^{+/+}$ mice. *Mlh1* heterozygous offspring were euthanized after genotyping. Experimental mice were monitored closely for 9 months, after which they were euthanized and autopsied. Mice that were moribund before 9 months were also euthanized and autopsied. Tumors that developed in these mice include lymphomas, skin tumors, intestinal adenomas, and adenocarcinomas. Tumor and tissue samples were dissected and snap frozen in liquid N_2, as well as paraffin embedded for histology.

DNA isolation. Genomic DNA was isolated from tumor samples and from tail biopsies of 4-week-old mice as described previously (47). Tissues were lysed in 100 mM Tris-HCl (pH 8.5)–5 mM EDTA–0.2% sodium dodecyl sulfate–200 mM NaCl–100 μg of proteinase K/ml overnight at 55°C with agitation, followed by isopropanol precipitation. The DNA was then spooled from the isopropanol and resuspended in 10 mM Tris-HCl–0.1 mM EDTA (47).

DNA recombination assays. DNA rearrangement of the immunoglobulin and T-cell receptor loci was analyzed in *Mlh1* wild-type and *Mlh1*$^{-/-}$ thymus, tail, and lymphoma tissues by PCR. We used seminested and nested PCR primers to analyze $D_{\beta1}J_{\beta1}$, $D_{\beta1}J_{\beta2}$, and $D_{\beta2}J_{\beta2}$ recombination at the T-cell receptor beta (TCRβ) locus (85). Immunoglobulin heavy-chain (IgH) DJ recombination was determined using degenerate PCR primers as described previously (73).

Bisulfite treatment and MethyLight analysis. Genomic DNA was converted with sodium metabisulfite (Sigma) by using a modification of the agarose bead method (62). Denatured genomic DNA was suspended by being mixed with 4% Seakem agarose (FMC Corp.) to form a bead, equilibrated with 5 M bisulfite for 14 h at 50°C, washed, and desulfonated with 0.2 M NaOH. Agarose beads were melted, diluted, and stored at −20 degrees until used. Detection and quantitation of DNA methylation by MethyLight was performed as described previously (16–19). We examined methylation levels at 5 different CpG island sites. For each reaction, we used PCR primer and fluorescent probe combinations that contain CpG sites such that amplification occurs only if those CpG sites are methylated and only if the DNA is completely converted with bisulfite. The fluorescent signal for each reaction was adjusted for DNA input by normalizing to two independent reference reactions (*Guca2* and *Lhx1*), for which the primer and probe sequences do not contain any CpGs and are therefore not dependent on the methylation status of the DNA. Methylation levels are expressed as a ratio of the input DNA-adjusted signal and the signal of a reference methylated DNA sample (16–19). This reference DNA was obtained by the in vitro methylation of genomic DNA derived from 129/sv J1 ES cell line (52) with *Sss1* methylase (New England Biolabs) and subsequent bisulfite conversion. The primer and probe sequences used for MethyLight analysis were as follows: for *Timp3*, forward, 5′-GAGAGGCGGTGGGCGTAG-3′; reverse, 5′-CGAAAATATAAACTAAACGCGTCCT-3′; probe, 6FAM-5′-CGATATACGCTACAACGACGTCCCACGA-3′-TAMRA; for *MyoD1*, forward, 5′-CGTGTTTCGATTTATTAGATTTGCG-3′; reverse, 5′-CATCCTCACGAACGCCTAAAC-3′; probe, 6FAM-5′-CCACGTACACCAAACGCGAATCCA-3′-TAMRA; for *Int4a*, forward 5′-CGAGGTGTAGATCGAGGTTTCG-3′; reverse, 5′-AATACCCGATTAACACCCCGA-3′; probe, 6FAM-5′-ACAACATCACCGCTTCCCGAAAAACG-3′-TAMRA; for *Mgmt*, forward, 5′-CGACACCCTTACGTCACACACT-3′; reverse, 5′-TAGTTCGAGGGTGTAAAGCGG-3′; probe, 6FAM-5′-AACCACGCCCCGCGTACCAA-3′-TAMRA; for *Cdkn2a*, forward, 5′-CGCGAGGAAAGCGAATTC-

3′; reverse, 5′-CGAAACCCCGACTTCCAA-3′; probe, 6FAM-5′-CCCGCACG TCATACACACGACCCT-3′-TAMRA; for *Lhx1*, forward, 5′-AGAGTGTTTG GAAGTTAGGTGAAGGT-3′; reverse, 5′-CACATTCATAAACACAAATTC ACACAAC-3′; probe, 6FAM-5′-CACAATCAACATCCCAAACATATTCAC CCA-3′-TAMRA; and for *Guca2*, forward 5′-GGTGTTGTGGTTTAGAAGG TTATGG-3′; reverse, 5′-ACCTTATCCTCAACTTCCAACATACC-3′; probe, 6FAM-5′-TCTCATCATCTTCTACAAACCAAAAC-3′-TAMRA. (Dyes used were 6-carboxyfluorescein [6 FAM] and 6-carboxy-tetramethylrhodamine [TAMRA]; CpG sites are underlined.)

RNA expression analysis. We used real-time, fluorescence-based reverse transcription-PCR (RT-PCR) (Taqman) to measure gene expression (17). Total RNA was isolated using the guanidinium isothiocyanate method (Ambion Total RNA). RNA samples were then treated with DNase I to remove contaminating DNA (Ambion DNA-free). Samples were reverse transcribed with random primers and SuperScript II reverse transcriptase (Gibco-BRL) as specified by the manufacturer. *Dnmt1* expression was normalized to glyceraldehyde-3-phosphate dehydrogenase (*Gapdh*), *histone H4*, and *Pcna* control reactions. For the lymphoma analyses, we analyzed 17 different transcripts, including 2 control RNA transcripts, *Gapdh* and *histone H4*. Specific gene expression was normalized to both *Gapdh* and *histone H4* expression to correct for RNA input and averaged. The primer and probe sequences were as follows: for *Dnmt1*, forward, 5′-CCA TGGTGCTGAAGCTCACA-3′; reverse, 5′-AGCACACCAAAGGTGCACTG-3′; probe, 6FAM-TAGCCCATGCGGACCAGGCAG-3′-TAMRA; for *Bmi-1*, forward, 5′-CTGGAGAAGAAATGGCCCAC-3′; reverse, 5′-CCCTCTGGTG ACTTCATCTTCAT-3′; probe, 6FAM-5′-CCTTTGAAATACAGAGTTCGGC CAACTTGC-3′-TAMRA; for *C-myc*, forward 5′-ACAGCAGCTCGCCCAAA TC-3′; reverse 5′-CGAGTCCGAGGAAGGAGAGA-3′; probe 6FAM-5′-ACC TCGTCCGATTCCACGGCC-3′-TAMRA; for *N-myc*, forward 5′-CTGGCGA GCTGATCCTCAA-3′; reverse, 5′-GGTGAGGGTGCAGCATAGTTG-3′; probe, 6FAM-5′-CGCTGTGTTCCCATCCATCAGCA-3′-TAMRA; for *Pim-1*, forward 5′-TTCGGCTCGGTCTACTCTGG-3′; reverse, 5′-CACGTGCTTAA TGGCCACC-3′; probe, 6FAM-5′-ATCCGCGTCGCCGACAACTTG-3′-TA MRA; for *Pim-2*, forward, 5′-GAACCGTGTGCTAGGCTGGT-3′; reverse, 5′-ACAGCAGCGCAACCTCAAGT-3′; probe, 6FAM-5′-CACCGTGTCAGACT CAGTCACCTGCC-3′-TAMRA; for *Frat1*, forward, 5′-AGCTCGTGCTCTCG GGAA-3′; reverse, 5′-CTGTAGCTGTCGCGAATGAAGT-3′; probe, 6FAM-5′-TGCGCACCGCCTCCTTGATG-3′-TAMRA; for *Frat3*, forward, 5′-CTTC ATTCGCGAGGGCTACA-3′; reverse 5′-CTGACAAAGGCCCGAGGA-3′; probe, 6FAM-5′-AGGCAAAGCTTCCCGCTCACTCG-3′-TAMRA; for *Gfi1*, forward, 5′-TGCCGCTCTCTGGACGA-3′; reverse 5′-CCAGCAAGACCGCT CCAT-3′; probe, 6FAM-5′-CCAGCCCTACACGCTGCCTTTCA-3′-TAMRA; for *C-abl*, forward, 5′-TCTCTTAGGAAGACCCGCCA-3′; reverse, 5′-GTCCA GAACCACACCCTTGG-3′; probe, 6FAM-5′-AGCGCATTGCCAGTGGCAC CAT-3′-TAMRA; for *Bcl2*, forward, 5′-CATCTTCTCCTTCCAGCCTGA-3′; reverse 5′-ACGTCCTGGCAGCCATCTC-3′; probe, 6FAM-5′-AGCAACCCAAT GCCCGCTGTG-3′-TAMRA; for *C-fos*, forward, 5′-CTTCTTGTTTCCGGCA TCATC-3′; reverse, 5′-AGGTCCACATCTGGCACAGAG-3′; probe 6FAM-5′-AGGCCCAGTGGCTCAGAGACCTCC-3′-TAMRA; for IAP, forward, 5′-GA GTTTGAAGGCATCCTTGATACC-3′; reverse, 5′-TTGATATCCTAGGCCC TGTAATGAA-3′; probe, 6FAM-5′-CCCAAAGCATGGCCCACCACA-3′-TA MRA; for *Line1*, forward, 5′-ATAGCGCTGAGTGCCTCCA-3′; reverse, 5′-T TGGGTGAATTTGCTTCCTTTT-3′; probe, 6FAM-5′-TCAAGCTGCTAGTA TGTGCTGTCTCCCGT-3′-TAMRA; for *Arf*, forward, 5′-GGTCGCAGGTTC TTGGTCA-3′; reverse, 5′-AAAACCCTCTCTTGGAGTGGG-3′; probe, 6FAM-5′-CCGCGCGCTGAATCCTCACA-3′-TAMRA; for *Cdkn2a*, forward, 5′-ACGACTGGGCGATTGGG-3′; reverse, 5′-TCCAGATGGCTCTCCTCGA GT-3′; probe, 6FAM-5′-CACTGAATCTCCGCGAGGAAAGCG-3′-TAMRA; for *B1* elements, forward 5′-CACGCCTTTAATCCCAGCAC-3′; reverse, 5′-G CTGGCCTCGAACTCAGAAAT-3′; probe, 6FAM-5′-CGCCTGCCTCTGCC TCCCG-3′-TAMRA; for endogenous long terminal repeat (LTR), forward, 5′-TCTTGCTTCTTACACTCTTGCTCC-3′; reverse 5′-CAGGAAGAACACCAC AGACCAG-3′; probe, 6FAM-5′-ATCTTCTGCGGCAAAACTTTATTGCTT ACATCTT-3′-TAMRA; for GADPH, forward, 5′-TTGTCAAGCTCATTTCC TGGTATG-3′; reverse, 5′-GCCATGTAGGCCATGAGGTC-3′; probe, 6FAM-5′-CCACCCTGTTGCTGTAGCCGTATTCATT-3′-TAMRA; for histone H4, forward, 5′-TCTCCGGCCTCATCTACGAG-3′; reverse, 5′-CGGATCACGTT CTCCAGGA-3′; probe, 6FAM-5′-CACCTTCAGCACACCGCGGGT-3′-TA MRA; and for PCNA, forward, 5′-GAGCAACTTGGAATCCCAGAAC-3′; reverse, 5′-ATGTGGCTAAGGTCTCGGCATA-3′; probe, 6FAM-5′-TGCAAAT TCACCCGACGGCATCTTTATTA-3′-TAMRA.

RESULTS

Effects of *Dnmt1* hypomorphic mutations on expression and DNA methylation levels. Five independent targeted mutations of the murine *Dnmt1* gene have been described so far. These have been designated $Dnmt1^N$ (52), $Dnmt1^S$ (49), $Dnmt1^C$ (49), $Dnmt1^{CHIP}$ (76), and $Dnmt1^{1\Delta o}$ (34), and they all differ in the targeted location within the gene and the degree of disruption of Dnmt1 activity. In this report, we made use of one of these mutations, $Dnmt1^N$, and another *Dnmt1* mutation that has not been previously described, which we refer to as $Dnmt1^R$ (for insertion to *Eco*RV site) (Fig. 1A). The $Dnmt1^N$ allele is known to be hypomorphic, with very low levels of RNA message and protein (49, 52). The residual protein is slightly reduced in size (49), suggesting that a modified Dnmt1 protein results from an alternative splicing event around the *neo* cassette insert. Homozygous $Dnmt1^{N/N}$ mouse embryos had 30% of their normal methyl cytosine content and died at mid-gestation (52). Since we had observed that $Dnmt1^{S/R}$ mice show reduced viability (data not shown), while $Dnmt1^{N/R}$ mice are fully viable, we hypothesized that the $Dnmt1^R$ allele may be expressed at a higher level than the $Dnmt1^N$ allele but at a lower level than the wild-type allele. This was investigated by quantitative RT-PCR analysis (Fig. 1B). The $Dnmt1^{N/R}$ mice show substantially lower expression levels than the $Dnmt1^{N/+}$ mice, which supports this hypothesis. If the $Dnmt1^R$ allele is indeed a hypomorphic allele, then this could potentially result in detectably lower levels of genomic DNA methylation in combination with the other hypomorphic allele, $Dnmt1^N$. Figure 1C shows a Southern blot analysis of genomic DNA obtained from tail biopsies, which was digested with the methylation-sensitive restriction enzyme *Hpa*II and hybridized with a centromeric minor satellite repeat probe (8). $Dnmt1^{R/+}$ and $Dnmt1^{N/+}$ genomic DNA samples did not show detectable levels of hypomethylation relative to $Dnmt1^{+/+}$ DNA. However, $Dnmt1^{N/R}$ DNA showed clear evidence of enhanced digestion of centromeric repeat sequences by *Hpa*II, indicating that these sequences have reduced levels of methylation in these mice. We did not observe an effect of *Mlh1* genotype on methylation levels (data not shown).

$Dnmt1^{R/R}$ mice were viable and developed normally, in contrast to $Dnmt1^{N/N}$ mice, which show extensive hypomethylation and embryonic lethality (52). $Dnmt1^{N/R}$ mutants were also viable and showed detectable hypomethylation at centromeric repeat sequences, although their DNA was not as severely hypomethylated as complete knockout $Dnmt1^{C/C}$ embryonic stem cell DNA (49) (Fig. 1C). This strongly indicates that expression, enzyme activity, or both are higher for $Dnmt1^R$ than $Dnmt1^N$. Additionally, this confirms that while Dnmt1 activity is necessary for viability, mice with reduced expression still develop properly (46, 52). Therefore, we can rank genotypes $Dnmt1^{+/+} > Dnmt1^{R/+} > Dnmt1^{N/+} > Dnmt1^{N/R} > Dnmt1^{N/N}$ in decreasing order of Dnmt1 expression.

Tumor incidence in Mlh1-deficient mice harboring *Dnmt1* mutations. Mice with *Dnmt1* hypomorphic alleles were crossed with animals carrying a null mutation in the mismatch repair gene *Mlh1* (3). These mismatch repair-deficient mice are prone to the development of a spectrum of tumors, including skin tumors, intestinal adenomas, and adenocarcinomas. 129Sv/Jae $Mlh1^{+/-}$ $Dnmt1^{R/+}$ females were mated with C57/BL6

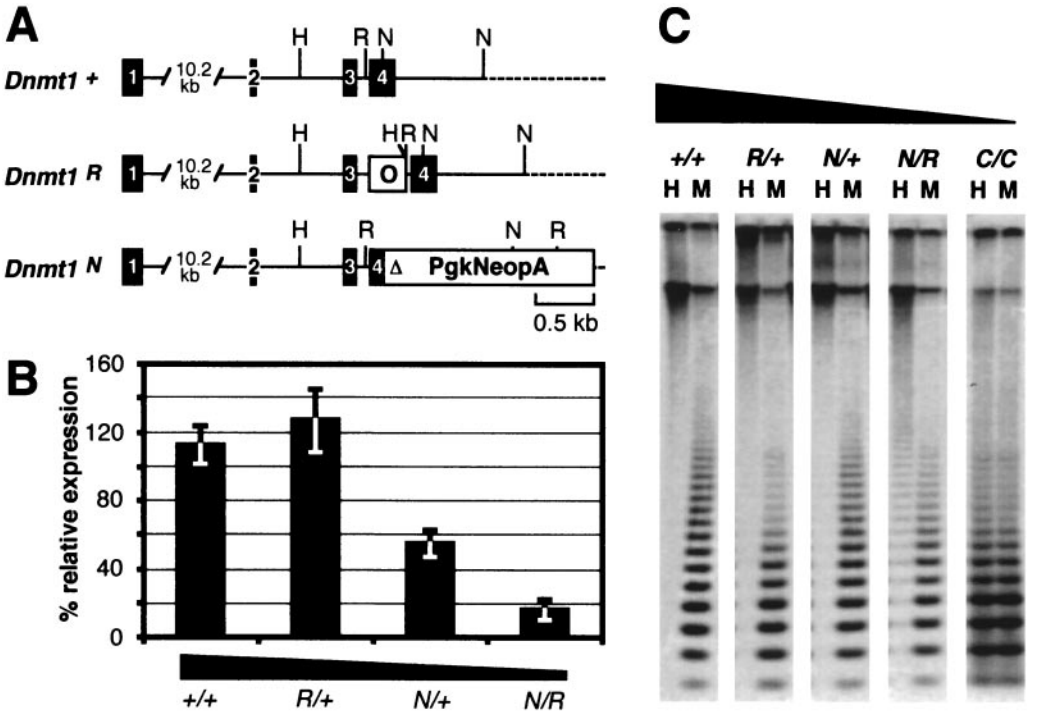

FIG. 1. Hypomorphic alleles of the mouse *Dnmt1* gene. (A) Schematic map (drawn approximately to scale) showing the positions of the *Dnmt1*^{R} and *Dnmt1*^{N} mutations in the 5′ region of the *Dnmt1* genomic locus. The first four exons shown are represented as numbered black boxes, and intervening introns are represented as solid lines. The 320-bp insertion (43, 44) containing three copies of the *lac* operator (*lacO*) sequence from *E. coli* is located just upstream of an *Eco*RV site (R) in intron 3 and is depicted as an open box (O). H, *Hin*dIII. The *Dnmt1*^{N} allele, which has been described previously (49, 52), contains a neomycin cassette that replaces a 900-bp *Nae*I (N) fragment. This mutation deletes part of exon 4 and causes an almost full disruption of *Dnmt1* expression. (B) *Dnmt1* expression in mutant mice as determined by real-time RT-PCR analysis. RNA was isolated from two thymus tissues of each genotype, and expression was normalized to expression of *Gapdh*, *histone H4*, and *Pcna*. The bars represent the mean value obtained for each of the normalized measurements shown on a relative scale. The error bars represent the standard error of the mean. The slope of the solid triangle below the graph schematically represents the relative Dnmt1 expression for each genotype. (C) DNA methylation of centromeric minor satellite repeats in *Dnmt1* mutant mice. Genomic DNA from tail biopsies of *Mlh1*$^{-/-}$ mice was digested with methylation-sensitive *Hpa*II (H) or with a methylation-insensitive isoschizomer, *Msp*I (M), as a control and then probed with a fragment derived from pMR150 (8). Results for DNA from a *Dnmt1*$^{C/C}$ complete-knockout embryonic stem cell line are shown as a control (49). Lower-molecular-weight bands in the *Hpa*II lanes indicate DNA hypomethylation. The slope of the solid triangle above the gels schematically represents the relative Dnmt1 expression for each genotype.

Mlh1$^{+/-}$ *Dnmt1*$^{N/+}$ males to produce 618 offspring. Of these, we obtained 30% *Dnmt1*$^{+/+}$, 26% *Dnmt1*$^{R/+}$, 23% *Dnmt1*$^{N/+}$, and 20% *Dnmt1*$^{N/R}$ ($P = 0.09$ by the chi-square test) and 25% *Mlh1*$^{+/+}$, 56% *Mlh1*$^{+/-}$, and 19% *Mlh1*$^{-/-}$ ($P = 0.02$ by the chi-square test). We observed that *Mlh1*$^{-/-}$ mice were underrepresented (19% [119 of 618]), in contrast to previous reports (3, 20). The 12 combinations of *Mlh1* and *Dnmt1* genotypes were obtained at expected frequencies (data not shown); this is consistent with the independent segregation of the two genes and indicates that the simultaneous absence of Mlh1 and reduced *Dnmt1* expression does not adversely affect development in mice. We monitored F_1 mice for 9 months, after which they were euthanized and assessed for tumors. We also euthanized mice that were moribund before 9 months and screened them for tumors that had developed (see Materials and Methods).

It has been suggested that DNA hypomethylation leads to an elevated rate of gene loss due to mitotic recombination and DNA rearrangement (10). We tested whether reduced *Dnmt1* expression by itself would increase tumorigenesis by examining *Mlh1*$^{+/+}$ mice with different *Dnmt1* genotypes. We euthanized 16 *Dnmt1*$^{+/+}$, 17 *Dnmt1*$^{R/+}$, 20 *Dnmt1*$^{N/+}$, and 22 *Dnmt1*$^{N/R}$ mice at 9 months, but autopsy failed to reveal tumors in any of these mice. Thus, it appears that the degree of hypomethylation in *Dnmt1*$^{N/R}$ DNA is insufficient to induce tumor formation in animals with proficient mismatch repair during the first 9 months.

We next assessed tumor susceptibility in mismatch repair-deficient *Mlh1*$^{-/-}$ animals. The Mlh1-deficient mice developed a spectrum of tumors similar to that described previously (22, 64). Lymphomas and intestinal tumors accounted for the vast majority of the observed tumors, but skin tumors were also seen in *Mlh1*$^{-/-}$ *Dnmt1*$^{+/+}$ mice. Of 24 *Mlh1*$^{-/-}$ *Dnmt1*$^{+/+}$ mice, 21% (5 of 24) developed aggressive lymphoid tumors, and 83% (20 of 24) developed either adenomas or adenocarcinomas in the intestinal tract by 9 months of age. One mouse developed a tumor of the uterine epithelium, and another had a skin tumor.

Tumor susceptibility in Mlh1-deficient mice was substantially modified when we crossed them with *Dnmt1* mutant mice (Fig. 2A and B). There was a strong effect of *Dnmt1* genotype on the frequency of intestinal tumors (Fig. 2A) and of lympho-

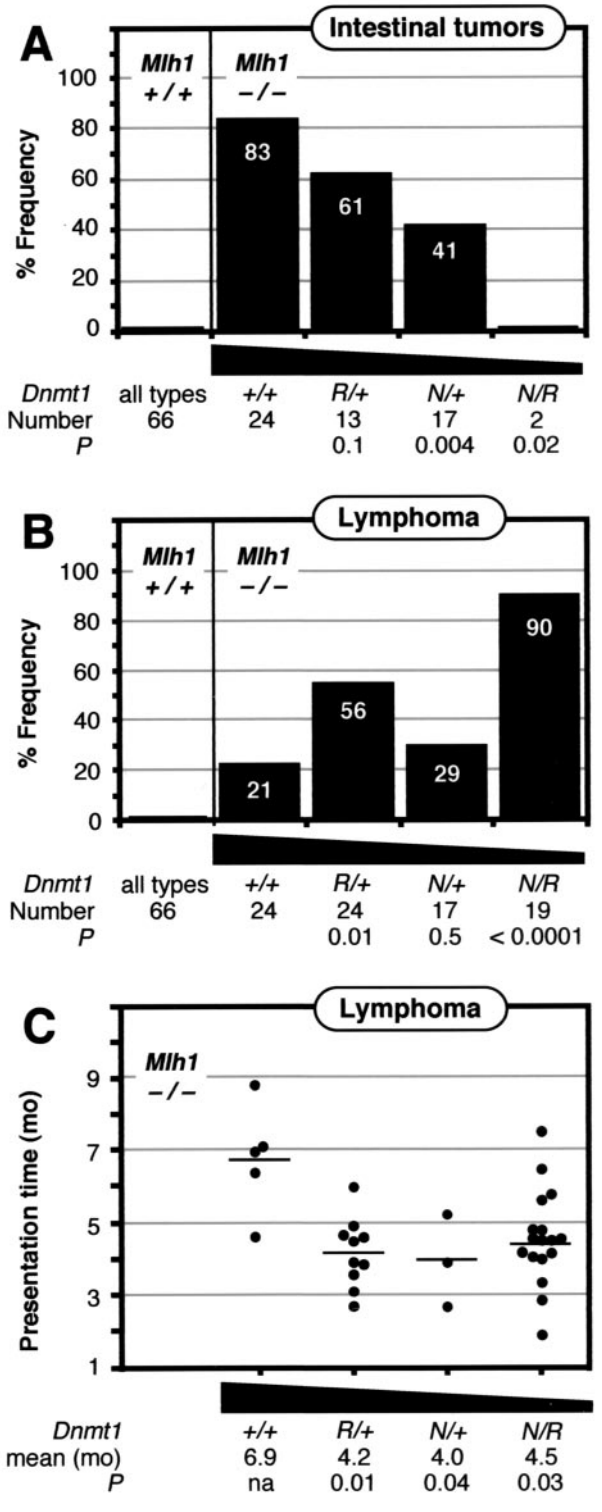

FIG. 2. Effect of *Dnmt1* mutations on the tumor incidence in Mlh1 deficient mice. (A) Effect of *Dnmt1* genotype on the cumulative frequency of intestinal tumors in Mlh1-deficient mice by 9 months of age. The number of mice in each cohort is shown at the bottom. The statistical significance of the difference in tumor frequency for each mutant genotype versus the wild type was tested using chi-square analysis, with the *P* values shown at the bottom. (B) Effect of *Dnmt1* genotype on the cumulative frequency of lymphomagenesis in Mlh1-deficient mice by 9 months of age. All F_1 Mlh1-deficient and wild-type mice were sacrificed when they were moribund or when they reached 9 months. The statistical significance of the difference in tumor frequency for each mutant genotype versus the wild type was tested using chi-square analysis, with the *P* values shown at the bottom. (C) Effect of *Dnmt1* genotype on the age of onset of lymphomas. The horizontal lines represent the mean age at diagnosis for each genotype. The statistical significance of the difference in age of onset of each mutant genotype versus wild-type mice was tested using an unpaired *t* test, with the *P* values shown at the bottom.

mas (Fig. 2B) in mice lacking Mlh1. In the intestinal epithelium, reduced Dnmt1 expression was associated with a diminished tumor burden (Fig. 2A). Figure 2A shows that at 9 months the cumulative frequency of intestinal tumors was 83% for $Dnmt1^{+/+}$ mice, but it decreased to 61% for $Dnmt1^{R/+}$ mice ($P = 0.1$) and to 41% for $Dnmt1^{N/+}$ mice ($P = 0.004$). There were two mice of the $Dnmt1^{N/R}$ genotype that survived to 9 months, and they did not develop any detectable intestinal tumors. These results suggest that mice with reduced Dnmt1 expression are less likely to develop intestinal tumors than *Dnmt1* wild-type littermates ($P = 0.02$ for trend). This reduced frequency of intestinal tumors in *Dnmt1* hypomorphic mice is not just an indirect consequence of increased lymphomagenesis (see below). The intestinal tumor incidence in just the surviving mice at 9 months was also reduced (71% for $Dnmt1^{+/+}$, 62% for $Dnmt1^{R/+}$ [$P = 0.36$], 44% for $Dnmt1^{N/+}$ mice [$P = 0.04$], and 0% for $Dnmt1^{N/R}$ mice [$P = 0.02$]). In contrast, lymphoma frequencies were dramatically elevated in these same mismatch repair-deficient *Dnmt1* mutant animals. As shown in Fig. 2B, $Dnmt1^{N/R}$ mutants were at highest risk of developing lymphomas (90% by 9 months versus wild type; $P < 0.0001$ by unpaired *t* test). $Dnmt1^{R/+}$ and $Dnmt1^{N/+}$ mice also developed lymphomas at higher frequencies ($P = 0.07$ for trend). In addition, *Dnmt1* mutant mice presented with lymphoma at a younger age than their $Dnmt1^{+/+}$ littermates, suggesting an enhanced rate of tumor formation in the lymphoid lineage (Fig. 2C). Consistent with a previous report (64), we found that the majority of $Mlh1^{-/-}$ $Dnmt1^{+/+}$ animals with lymphoma presented after 6 months. The mean age of onset of lymphomagenesis was significantly reduced in mice with any combination of *Dnmt1* hypomorphic alleles. Interestingly, we found that the lymphoma frequency was higher in $Dnmt1^{R/+}$ than in $Dnmt1^{N/+}$ mice.

Since this experiment was conducted in a syngeneic genetic background (F_1; 129sv/Jae and C57BL6), the observed tumor predisposition is modified specifically by *Dnmt1* genotype and not by strain differences. The effect on tumor frequency is tissue dependent. In the intestinal mucosa, the effect appears to be protective against adenomas and adenocarcinomas. In the lymphoid lineage, the tumor burden is enhanced by *Dnmt1* mutations. To our knowledge, this is the first report showing that a reduction in Dnmt1 expression concomitantly exacerbates and diminishes tumor incidence in different tissues.

Effects of *Dnmt1* genotype on survival of Mlh1-deficient mice. Mlh1-deficient mice are known to have reduced survival (64). We confirmed this in our study as well (Fig. 3). At 9 months, all of the 16 $Mlh1^{+/+}$ $Dnmt1^{+/+}$ mice we examined were still alive, but only 65% (22 of 34) of the $Mlh1^{-/-}$ $Dnmt1^{+/+}$ mice had survived. *Dnmt1* hypomorphic alleles showed an interesting interaction with $Mlh1^{-/-}$ homozygosity.

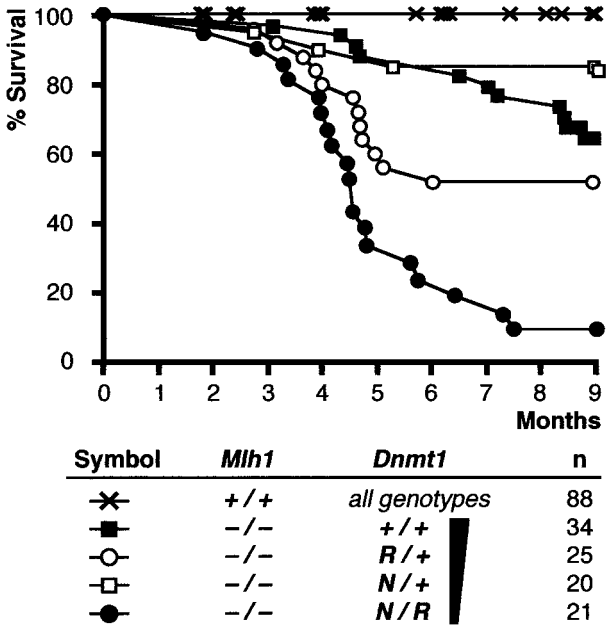

FIG. 3. Kaplan-Meier survival curves of Mlh1-deficient, *Dnmt1* mutant mice up to 9 months. *n*, number of mice in each genotype cohort. Each group was monitored closely for 9 months, at which time mice were euthanized and examined on autopsy. Each point represents a death event for a mouse, which is then censored from further survival analysis. Mice removed from cohorts for any other reasons were also censored so that only the survival data for the remaining cohort is monitored.

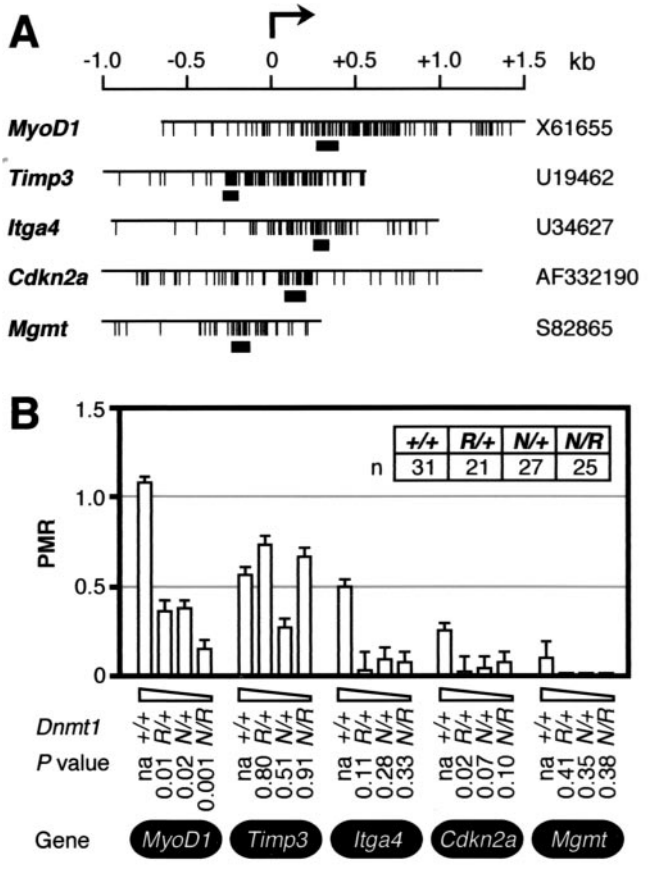

FIG. 4. MethyLight analysis of five CpG islands. (A) CpG density maps of five CpG islands analyzed by MethyLight. Individual CpG sites are indicated by vertical lines. Locations of MethyLight amplicons are indicated by solid boxes. Sequences are aligned relative to their respective transcriptional starts at position 0, indicated by the arrow pointing to the right. GenBank accession numbers are indicated to the right of the CpG density maps. (B) MethyLight analysis of CpG island hypermethylation in normal mucosal tissue. Genomic DNA from jejunum mucosal tissue was bisulfite converted and then used to measure CpG island hypermethylation. CpG island hypermethylation is expressed as percentage of methylated reference (PMR) value (19). The calculation of PMR values is described in Materials and Methods. Geometric means of the PMR values were calculated, since the methylation data are not normally distributed. The error bars represent the standard errors of the means. The statistical significance of the difference in CpG island hypermethylation for each gene of each mutant genotype versus the wild type was tested using the Mann-Whitney U test, with the *P* values shown at the bottom.

Dnmt1$^{N/R}$ mice had the poorest survival due to the accelerated lymphomagenesis. *Dnmt1* wild-type mice survived best early on, but they dropped below *Dnmt1*$^{N/+}$ mice in survival rates later in life, due to their higher rates of intestinal tumorigenesis (Fig. 3). Our results suggest that lowering Dnmt1 expression levels can substantially affect longevity of Mlh1-deficient mice through modification of tumor burden risks. As *Mlh1*$^{+/+}$ *Dnmt1* mutant animals did not show reduced survival, a decrease in Dnmt1 expression by itself has little effect on longevity until it is coupled with additional molecular deficiencies such as a loss of mismatch repair.

Methylation analysis of DNA from intestinal tumors. The reduced frequency of intestinal tumors in *Dnmt1* hypomorphic mice suggests that Dnmt1, or its resulting methylation, may contribute to tumorigenesis in the intestinal mucosa. Dnmt1 could potentially participate in oncogenesis by mediating hypermethylation of promoter CpG islands (38). Hypermethylation of some genes, such as tumor suppressors, would be expected to predispose the intestinal mucosa to oncogenic transformation. The occurrence of occasional CpG island hypermethylation in the normal mucosa would thus be expected to predispose some cells to neoplastic transformation. Therefore, we used the sensitive MethyLight assay (16–19) to determine whether CpG island hypermethylation could be detected in the normal intestinal mucosa of *Dnmt1* hypomorphic mice (Fig. 4B). The MethyLight assay is well suited for this analysis, since it can detect very low occurrences of fully methylated CpG islands (16–19). Such fully methylated CpG islands are expected most likely to result in transcriptional silencing of the associated gene. We chose a collection of CpG islands that included both genes implicated in oncogenesis (*Cdkn2a*) and those thought to be neutral to the process (*Myod1*), so that we could assess whether any observed CpG island hypermethylation was a generalized phenomenon or was restricted to genes providing a selective advantage (Fig. 4A). We isolated genomic DNA from normal mucosa or tumors, performed sodium bisulfite conversion, and analyzed methylation levels for the genes *Myod1*, *Timp3*, *Itga4*, *Cdkn2a* (*p16*), and *Mgmt*. We performed MethyLight analysis of DNA from normal mucosa of *Dnmt1* mutant mice to determine if there were significant methylation differences in the normal mucosa between the various *Dnmt1*

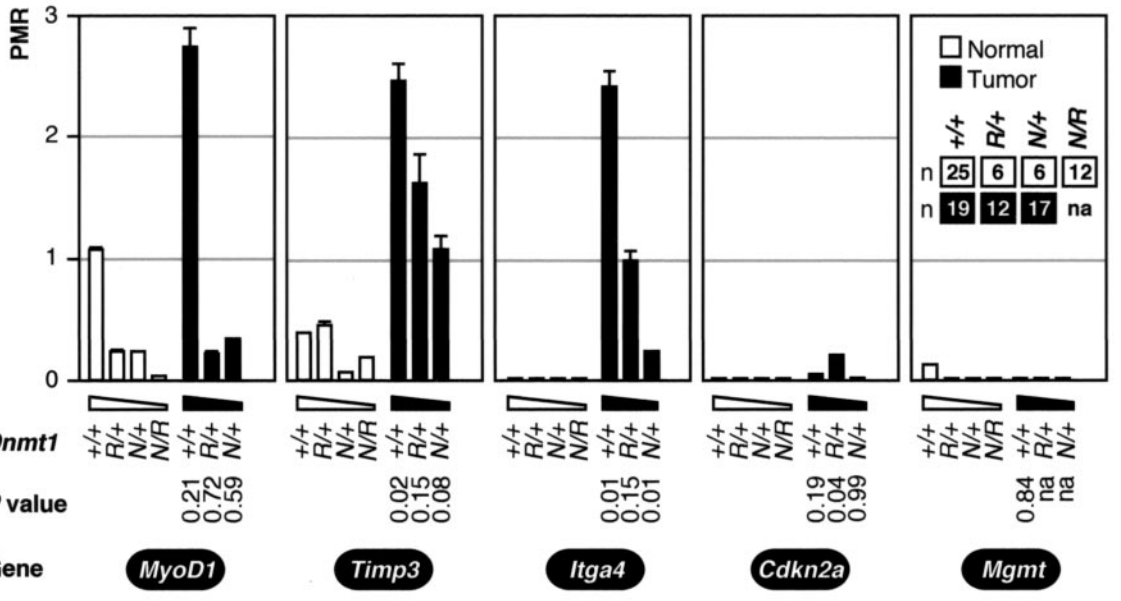

FIG. 5. MethyLight analysis of CpG island hypermethylation at five sites in normal mucosa and intestinal tumors of *Mlh1*$^{-/-}$ mice. Genomic DNA from jejunum mucosal tissue or tumor tissue was bisulfite converted and then used to measure CpG island hypermethylation. CpG island hypermethylation is expressed as percentage of methylated reference (PMR) value (19). The calculation of PMR values is described in Materials and Methods. Geometric means of the PMR values were calculated, since the methylation data are not normally distributed. The error bars represent the standard errors of the means. The statistical significance of the difference in CpG island hypermethylation between normal and tumor tissue was tested separately for each gene and for each genotype using the Mann-Whitney U test, with the *P* values shown at the bottom.

genotypes (Fig. 4B). We found a trend of decreasing methylation in the *Dnmt1* mutant mice at genes *Myod1*, *Itga4*, *Cdkn2a*, and *Mgmt*. CpG island hypermethylation was generally highest in the intestinal mucosa of *Dnmt1* wild-type mice. The effect of *Dnmt1* genotype on DNA methylation levels was most pronounced for *MyoD1*. At this locus, there was a strong, statistically significant difference in methylation between *Dnmt1*$^{+/+}$ DNA and DNA from other *Dnmt1* mutant genotypes. The greatest difference was seen between *Dnmt1*$^{+/+}$ and *Dnmt1*$^{N/R}$ ($P = 0.001$ by the Mann-Whitney U test; nonparametric statistical tests were used, since the methylation data are not normally distributed). We also observed a significant decrease of methylation levels in the *Dnmt1* mutant mice at *Cdkn2a* ($P = 0.02$ for *Dnmt1*$^{+/+}$ versus *Dnmt1*$^{R/+}$). We did not detect an effect of genotype on methylation levels at *Timp3*, suggesting that this locus is resistant to changes in Dnmt1 activity or that other methyltransferases contribute to methylation at this genomic location. Our results suggest that Dnmt1 contributes to methylation at these CpG islands in the normal mucosa, which could cause a predisposition to neoplastic progression. If this is indeed the case, then one would expect CpG island hypermethylation levels to be higher in the resulting intestinal tumors than in the originating normal mucosa, which consists of many cells without any or with lower levels of CpG island hypermethylation. We therefore investigated whether CpG island hypermethylation was elevated in the intestinal tumors of Mlh1-deficient mice with different Dnmt1 genotypes (Fig. 5).

We observed a tendency for tumor DNA to have higher levels of CpG island hypermethylation at three of the five genes analyzed. This is apparent at genes *Timp3*, *Myod1*, and *Itga4*, at which CpG island hypermethylation levels were higher in the tumor DNAs than in their corresponding normal mucosal samples. The difference between tumor and normal tissues was statistically significant for *Timp3* and *Itga4* for *Dnmt1*$^{+/+}$ animals ($P = 0.02$ at *Timp3* and $P = 0.01$ at *Itga4*). To our knowledge, this is the first demonstration of increased CpG island hypermethylation of intestinal tumors in mice. CpG island hypermethylation was also observed in tumors derived from *Dnmt1*$^{R/+}$ and *Dnmt1*$^{N/+}$ mice for the genes *Timp3*, *Itga4*, and *Cdkn2a*, although it was less pronounced than in *Dnmt1*$^{+/+}$ tumors. We could not perform a similar test for the mice of the *Dnmt1*$^{N/R}$ genotype, because these animals did not develop intestinal tumors.

It is interesting that tumor CpG island hypermethylation decreased by *Dnmt1* genotype, just as in the normal intestinal mucosa. This suggests that the low rate of tumorigenesis that does occur in *Dnmt1* hypomorphic mice may rely less on CpG island hypermethylation. Presumably, other oncogenic mechanisms that are less dependent upon Dnmt1 expression predominate in mice with limiting amounts of Dnmt1. The reduced rates of intestinal tumorigenesis in *Dnmt1* hypomorphic mice may be a consequence of the limited capacity for CpG island hypermethylation in these mice, although we do not have direct evidence for this. We observed a correlation between CpG island hypermethylation frequency and rates of intestinal tumorigenesis, but this is not proof of a causal link.

Analysis of lymphoid tumors from Mlh1-deficient mice. Previous studies have reported that mismatch repair-deficient mice are predisposed to the development of lymphomas, including T-cell lymphomas in *Msh2* knockout mice and both B- and T-cell lymphomas in *Msh6* mutant mice (15, 20). *Mlh1* and

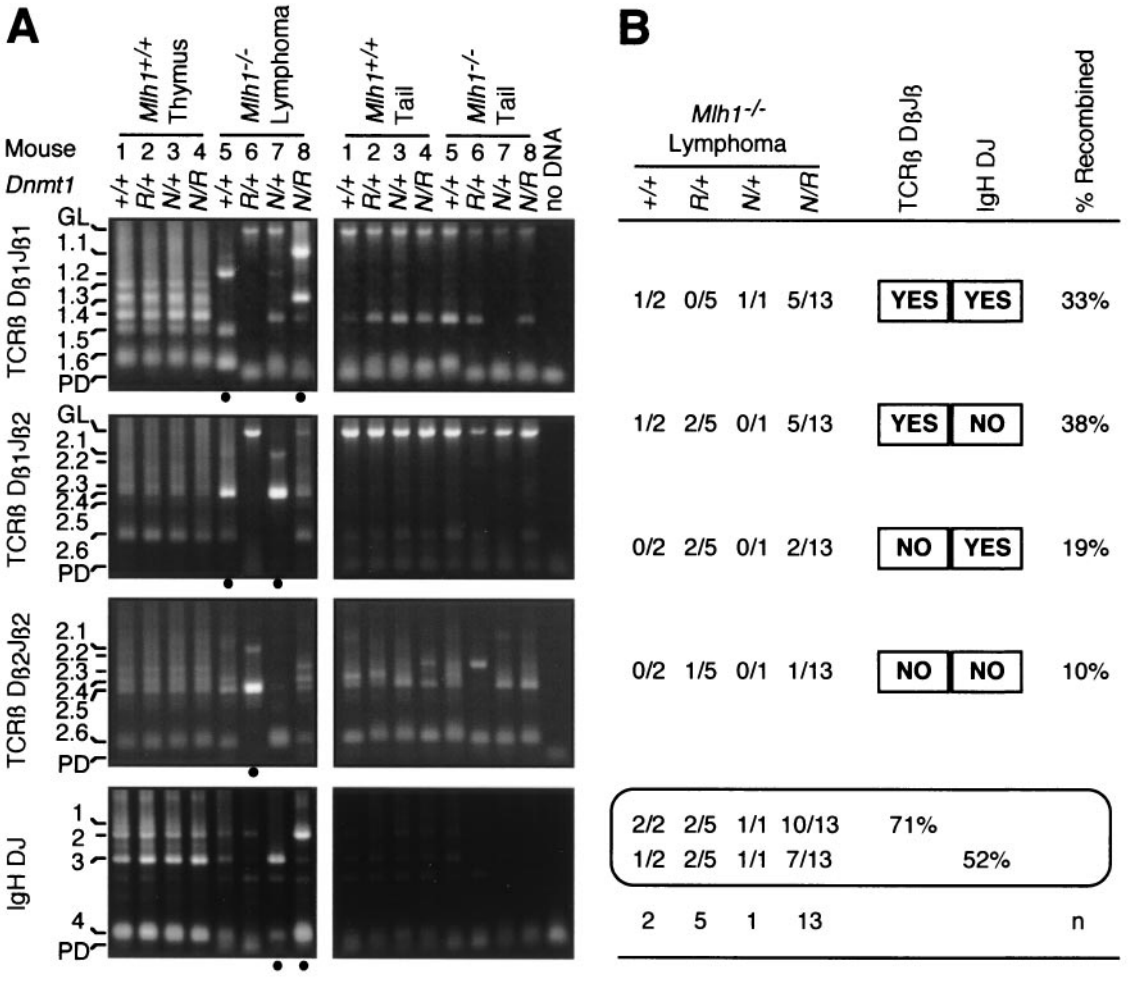

FIG. 6. Recombination of lymphoma DNA in Mlh1-deficient, *Dnmt1* mutant mice. (A) $D_{\beta1}J_{\beta2}$ and $D_{\beta1}J_{\beta2}$ recombinations at the TCRβ locus and DJ recombination at the IgH locus were determined using PCR of genomic DNAs derived from various tissues, and products were separated on an agarose electrophoresis gel (85). Representative DNA samples from four *Mlh1* wild-type thymus samples (lanes 1 to 4, left panels) and four lymphoma samples (lanes 5 to 8, left panels) at each *Dnmt1* genotype and their matched control tail DNAs are shown. Lanes with thymus DNA show different possible DJ configurations, while some lanes with lymphoma DNA show one or two predominant configurations (indicated by a closed circle below the lane). Recombined product bands seen in the tail DNA lanes (right panel) are due to DNA from blood lymphocytes that contaminated the samples. GL, unrearranged, germ line configuration; PD, primer dimer. (B) Summary of DNA recombination in lymphoma in Mlh1-deficient mice for each *Dnmt1* genotype.

Pms2 mutant mice also succumb to lymphomas, but their phenotypes were not reported (3, 20). The vast majority of lymphoid tumors that we observed in our mouse colony presented in the thymus, suggesting that they may be of the T-cell lineage. Splenomegaly was occasionally observed in conjunction with a thymoma. We characterized these lymphomas by using PCR to analyze DJ recombination at the TCRβ locus and at the IgH locus (Fig. 6). Out of 21 lymphoma samples tested, 19 (90%) showed a dominant recombined band (Fig. 6A) when tested for either TCRβ or IgH. DJ rearrangement at TCRβ was detected in 71% (15 of 21) of the tumors, while rearrangement at IgH was seen in 52% (11 of 21) of the tumors. This is consistent with the observation that the majority of these tumors developed in the thymus and would therefore be expected to be of the T-cell lineage. DJ recombination at these two loci was not mutually exclusive, as 33% (7 of 21) of these samples showed simultaneous DNA rearrangements at both TCRβ and IgH. Due to the small sample size, we could not determine if the *Dnmt1* genotype had an effect on these recombination frequencies. We did not observe dominant recombined bands in any of the control thymus DNA or matched tail DNA samples (Fig. 6A) when assayed at either TCRβ or IgH.

We next investigated the mechanism by which reduced levels of *Dnmt1* expression might have resulted in enhanced rates of lymphomagenesis in Mlh1-deficient mice. It does not appear that the effects of *Dnmt1* hypomorphic alleles on the rates of lymphomagenesis are exerted primarily through CpG island hypermethylation, since lymphomagenesis is increased in these mice, while CpG island hypermethylation is decreased. Since retroviral infection and proviral activation of proto-oncogenes are known to cause lymphomas in mice (6, 79, 80), we hypothesized that *Dnmt1* mutant mice might have increased rates of endogenous proviral activation, or increased expression of

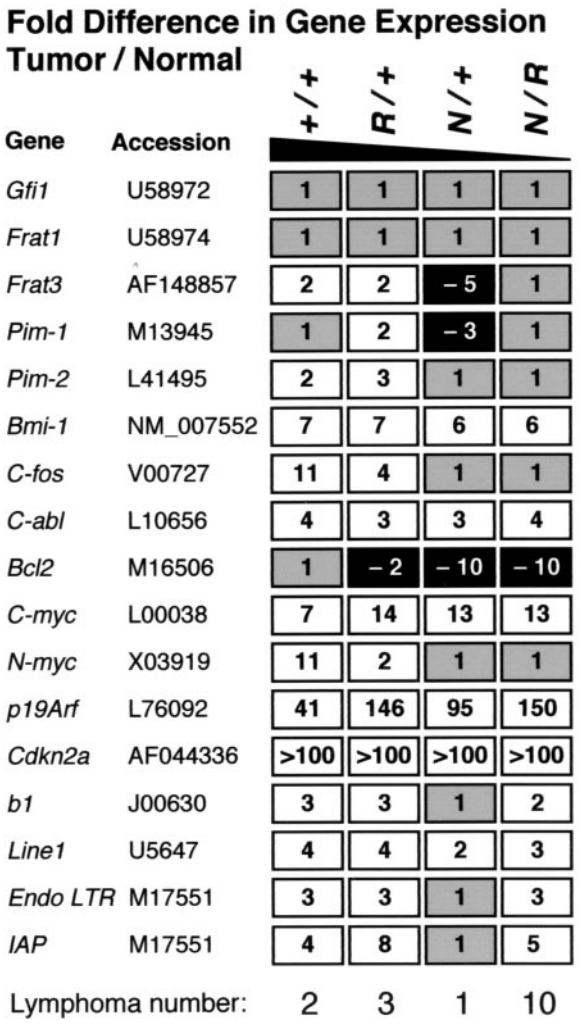

FIG. 7. Summary of genes induced (white boxes), repressed (black boxes), or unchanged (gray boxes) in lymphoid tumors from Mlh1-deficient mice. Gene expression levels of 17 transcripts were analyzed using real-time RT-PCR in lymphomas (the number is indicated at the bottom of the chart) and compared to the mean values for eight age-matched normal thymus tissues from Mlh1 wild-type mice. Gene expression was normalized to both *Gapdh* and *histone H4* expression to correct for RNA input and averaged. The values shown in each box represent the relative increase or decrease in expression level in the lymphomas versus the control tissues.

proto-oncogenes, due to reduced levels of promoter methylation. To test this, we analyzed the expression of 17 different genes and repetitive elements in lymphoma samples by using real-time fluorescence-based Taqman RT-PCR (Fig. 7). The level of expression of each of the 17 transcripts in the lymphomas was calculated relative to the expression level in corresponding $Mlh1^{+/+}$ thymus control samples. We found that 10 out of 17 transcripts showed a significant difference in expression between lymphoma and thymus samples in at least one of the *Dnmt1* genotypes. On average, many of the tested genes and repeat elements showed upregulation in lymphoma tissues. There was a significantly elevated expression of the *C-abl*, *Bmi-1*, *C-myc*, and *N-myc* genes. These genes (with the exception of *C-abl*) have been shown to be activated by proviral insertion in Moloney murine leukemia virus-induced lymphoma models (6, 79, 80). Our analysis did not reveal upregulation of some other oncogenes that have been shown to be overexpressed in lymphoma models (e.g., *Gfi1* and *Frat-1*). Interestingly, we found that the tumor suppressor genes *p19Arf* and *Cdkn2a* both showed strongly increased expression levels in lymphoid tumors relative to control tissues. *Bcl2* was the only gene to show a reduced level of expression in lymphomas compared to normal thymus.

Although the expression levels of *IAP* and endogenous *LTR* elements were modestly enhanced in $Dnmt1^{R/+}$ and $Dnmt1^{N/R}$ mice, we did not observe a strong and convincing difference in gene upregulation between the different *Dnmt1* genotypes. This implies that similar lymphomagenic pathways are utilized in mice with different *Dnmt1* genotypes. Since the rate of lymphomagenesis is higher in *Dnmt1* hypomorphic mice, this may indicate that the oncogenic pathways shared by these mice are activated more readily in animals with reduced levels of *Dnmt1* expression but that the relative contribution of each of the pathways does not shift in the *Dnmt1* hypomorphs. In other words, the nature of the lymphomagenic process has not been altered by reduced *Dnmt1* expression, but the rate at which these processes are activated or proceed has increased.

DISCUSSION

Mice carrying germ line mutations of the *Mlh1* mismatch repair gene have both an enhanced mutational burden (100- to 1,000-fold increase) and a greater tumor incidence (22, 64). Our results clearly demonstrate that hypomorphic mutations of *Dnmt1* differentially affect neoplastic development in two separate tissue compartments, as was illustrated by an exacerbated tumor frequency in lymphoid tissues and a diminished tumor frequency in the intestinal epithelium in *Dnmt1* mutant, Mlh1-deficient mice. The protection from intestinal tumors in *Dnmt1* mutant animals may be a consequence of reduced CpG island-associated promoter hypermethylation, while the enhanced lymphomagenesis in the same animals may be the result of overexpression of endogenous retroviruses and/or proto-oncogenes or a consequence of an increase in genomic rearrangements.

It is generally thought that global DNA hypomethylation and silencing of growth control genes by promoter hypermethylation contribute to cancer progression (38). However, the causal role of these abnormal epigenetic changes in cancer development is sometimes unclear, since they could either directly contribute to neoplastic transformation or simply be a consequence of the malignant transformation. Promoter CpG island hypermethylation has been shown to interfere with transcription by causing the local chromatin to form a compact, transcriptionally repressed state through the recruitment of methyl-binding proteins, histone deacetylase, and corepressors (26, 39, 57–59, 67). Some studies involving mouse embryonic stem cells with reduced Dnmt1 expression and patients with immunodeficiency, centromeric region instability, and facial anomaly syndrome support the hypothesis that DNA hypomethylation can increase cancer risk by enhancing chromosomal instability (10, 28, 60, 87). However, we and others have also reported that DNA hypomethylation can suppress tumorigen-

esis and lead to reduced rates of gene inactivation (7, 12, 46, 55, 65). In light of our findings, one could argue that the effects of reduced methylation levels depend on the tissue origin of the tumor. Indeed, our results suggest that DNA hypomethylation can concomitantly enhance and diminish tumor development.

This study relies on the use of two *Dnmt1* hypomorphic alleles. Although the molecular and phenotypic studies indicate that the expression from these alleles is below wild-type levels, the precise mechanism by which this is achieved is not fully clear. It appears that both of these hypomorphic mutations cause a reduced expression at the RNA level by interfering with efficient and correct splicing, leading to an accompanying decrease in protein levels. The transcript generated from the *Dnmt1*^{R} allele appears to be normal in length and sequence composition but present at lower-than-wild-type levels.

Although we observed clear effects of *Dnmt1* hypomorphic alleles on tumorigenesis in mismatch repair-deficient animals, we cannot conclude that this effect is a direct consequence of reduced levels of DNA methylation. It is now known that the Dnmt1 protein itself is associated with activities that are distinct from the enzymatic ability of Dnmt1 to methylate DNA (11, 26, 41, 67, 72). Therefore, the effect of reduced levels of Dnmt1 on tumorigenesis may be a consequence of alterations in the transcriptional repressive complexes associated with Dnmt1, rather than being due to changes in genomic DNA methylation levels.

We found a good correlation between predicted Dnmt1 expression levels and intestinal tumorigenesis (Fig. 2A). These results are consistent with previous studies documenting suppression of polyp multiplicity in *Apc*^{Min} mice by *Dnmt1* mutations and 5-azadeoxycytidine treatment (12, 46). On the other hand, we did not observe a perfect correlation between predicted Dnmt1 expression levels and lymphomagenesis, since the lymphoma incidence in *Dnmt1*$^{N/+}$ mice was lower than that in the *Dnmt1*$^{R/+}$ mice (Fig. 2B). This result could be due to a statistical aberration, or it may reflect a dominant activity by a truncated form of the Dnmt1 protein expressed by one of the hypomorphic alleles. Further experiments will be needed to investigate whether this result is reproducible, and if so, what the molecular mechanism is that is responsible for this finding.

We suggest that the mechanism of intestinal tumor suppression by Dnmt1 hypomorphic alleles is through a reduced frequency of CpG island hypermethylation in the normal mucosa and during intestinal tumor formation. We provide evidence that *Dnmt1* mutant mice have a reduced frequency of CpG island hypermethylation in both normal mucosal and tumor DNAs, as determined for a limited number of CpG islands. We do not believe that the five loci that we analyzed are necessarily involved in intestinal tumor formation, but we suggest that the process of CpG island hypermethylation does occur in the mouse intestinal mucosa, that it is increased in intestinal tumors, and that it is suppressed in *Dnmt1* hypomorphic mice.

Since Mlh1-deficient mice are already subjected to greatly elevated mutation rates, it seems unlikely that Dnmt1 insufficiency would contribute substantially to lymphomagenesis by further increasing the mutation rate. Rather, the observed acceleration of lymphomagenesis in *Mlh1*$^{-/-}$ mice by *Dnmt1* hypomorphic alleles is likely to be due to an additive or synergistic effect of mismatch repair deficiency and DNA methyltransferase insufficiency through different mechanisms. In particular, our data do not provide evidence for a direct interaction between the mismatch repair process and DNA methylation, since functional mismatch repair is presumed to be absent in *Mlh1*$^{-/-}$ mice. It is possible that *Dnmt1* mutations lead to an increased MSI by enhancing DNA polymerase slippage or misincorporation rates, but there is no evidence to support this. It seems more likely that the enhanced lymphomagenesis is a consequence of an increased rate of the same type of endogenous retroviral or proto-oncogene activation or chromosomal instability that occurs normally in *Mlh1*$^{-/-}$-induced lymphomas. We did find evidence for increase expression of some proto-oncogenes and also of endogenous LTR elements and IAP in our lymphoid tumors. Endogenous IAP and related repetitive viral elements are normally silenced by dense methylation (82) but can be induced to reactivate by hypomethylation and thereby could afford higher rates of de novo integration which then could either disrupt genes or cause constitutive gene activation. However, since only a few lymphoid tumors per genotype were available for analysis, we could not definitively show that hypomethylation induces lymphomagenesis through an endogenous retroviral reactivation mechanism. An alternative view is that hypomethylation enhances lymphomagenesis by directly allowing proto-oncogenes to be expressed at higher levels. A recent study showed that up to 10% of genes are abnormally expressed in Dnmt1-deficient cells (36). Thus, the risk of developing lymphoma could be greatly exacerbated by a combination of mismatch repair deficiency, aberrant gene expression and the inherent chromosomal instability that is proposed to be associated with a hypomethylated genome (10, 28, 60, 87).

Finally, it is yet unclear if our observations can be readily extended to human cancer. The opposing effects of DNA hypomethylation on tumorigenesis are interesting and potentially relevant to human clinical trials of methyltransferase inhibitors. Inhibition of Dnmt1 activity could be effective in the prevention of colorectal cancer in at-risk individuals with familial adenomatous polyposis or hereditary nonpolyposis colorectal cancer. We had previously shown that reduced Dnmt1 expression can suppress polyp formation in a mouse model of familial adenomatous polyposis (46). In this study, we now also provide evidence that reduced Dnmt1 expression can inhibit intestinal tumor formation in a mouse model of hereditary nonpolyposis colorectal cancer. Drugs such as 5-azacytidine and 5-aza-2′-deoxycytidine are in clinical trials for the treatment of various hematopoietic and solid malignancies but are considered too toxic and mutagenic for long-term preventive therapy (37). Thus, development of less toxic inhibitors of Dnmt1 may be beneficial in the treatment and prevention of colorectal cancer. However, our finding of increased rates of lymphomagenesis in Dnmt1 hypomorphic mice suggests that long-term inhibition of DNA methyltransferases in humans may have an associated increased lymphoma or leukemia risk. Obviously, there are important differences between the mouse and human tumor systems. Nevertheless, our results offer new insights into the tissue-dependent balance of oncogenic effects of Dnmt1 expression levels.

ACKNOWLEDGMENTS

This work was supported by NIH/NCI grant R01 CA 75090 to P.W.L.

We thank Michael Liskay for providing *Mlh1* knockout mice.

REFERENCES

1. **Ahuja, N., A. L. Mohan, Q. Li, J. M. Stolker, J. G. Herman, S. R. Hamilton, S. B. Baylin, and J. P. Issa.** 1997. Association between CpG island methylation and microsatellite instability in colorectal cancer. Cancer Res. **57:**3370–3374.
2. **Baker, S. M., C. E. Bronner, L. Zhang, A. W. Plug, M. Robatzek, G. Warren, E. A. Elliott, J. Yu, T. Ashley, N. Arnheim, et al.** 1995. Male mice defective in the DNA mismatch repair gene PMS2 exhibit abnormal chromosome synapsis in meiosis. Cell **82:**309–319.
3. **Baker, S. M., A. W. Plug, T. A. Prolla, C. E. Bronner, A. C. Harris, X. Yao, D. M. Christie, C. Monell, N. Arnheim, A. Bradley, T. Ashley, and R. M. Liskay.** 1996. Involvement of mouse Mlh1 in DNA mismatch repair and meiotic crossing over. Nat. Genet. **13:**336–342.
4. **Baylin, S. B., and J. G. Herman.** 2000. DNA hypermethylation in tumorigenesis: epigenetics joins genetics. Trends Genet. **16:**168–174.
5. **Bellacosa, A., L. Cicchillitti, F. Schepis, A. Riccio, A. T. Yeung, Y. Matsumoto, E. A. Golemis, M. Genuardi, and G. Neri.** 1999. MED1, a novel human methyl-CpG-binding endonuclease, interacts with DNA mismatch repair protein MLH1. Proc. Natl. Acad. Sci. USA **96:**3969–3974.
6. **Berns, A., N. van der Lugt, M. Alkema, M. van Lohuizen, J. Domen, D. Acton, J. Allen, P. W. Laird, and J. Jonkers.** 1994. Mouse model systems to study multistep tumorigenesis. Cold Spring Harbor Symp. Quant. Biol. **59:**435–447.
7. **Chan, M. F., R. van Amerongen, T. Nijjar, E. Cuppen, P. A. Jones, and P. W. Laird.** 2001. Reduced rates of gene loss, gene silencing, and gene mutation in dnmt1-deficient embryonic stem cells. Mol. Cell. Biol. **21:**7587–7600.
8. **Chapman, V., L. Forrester, J. Sanford, N. Hastie, and J. Rossant.** 1984. Cell lineage-specific undermethylation of mouse repetitive DNA. Nature **307:**284–286.
9. **Chen, D., C. L. Luongo, M. L. Nibert, and J. T. Patton.** 1999. Rotavirus open cores catalyze 5′-capping and methylation of exogenous RNA: evidence that VP3 is a methyltransferase. Virology **265:**120–130.
10. **Chen, R. Z., U. Pettersson, C. Beard, L. Jackson-Grusby, and R. Jaenisch.** 1998. DNA hypomethylation leads to elevated mutation rates. Nature **395:**89–93.
11. **Chuang, L. S., H. I. Ian, T. W. Koh, H. H. Ng, G. Xu, and B. F. Li.** 1997. Human DNA-(cytosine-5) methyltransferase-PCNA complex as a target for p21WAF1. Science **277:**1996–2000.
12. **Cormier, R. T., and W. F. Dove.** 2000. Dnmt1N/+ reduces the net growth rate and multiplicity of intestinal adenomas in C57BL/6-multiple intestinal neoplasia (Min)/+ mice independently of p53 but demonstrates strong synergy with the modifier of Min 1(AKR) resistance allele. Cancer Res. **60:**3965–3970.
13. **Cui, H., I. L. Horon, R. Ohlsson, S. R. Hamilton, and A. P. Feinberg.** 1998. Loss of imprinting in normal tissue of colorectal cancer patients with microsatellite instability. Nat. Med. **4:**1276–1280.
14. **de Vries, S. S., E. B. Baart, M. Dekker, A. Siezen, D. G. de Rooij, P. de Boer, and H. te Riele.** 1999. Mouse MutS-like protein Msh5 is required for proper chromosome synapsis in male and female meiosis. Genes Dev. **13:**523–531.
15. **de Wind, N., M. Dekker, A. Berns, M. Radman, and H. te Riele.** 1995. Inactivation of the mouse Msh2 gene results in mismatch repair deficiency, methylation tolerance, hyperrecombination, and predisposition to cancer. Cell **82:**321–330.
16. **Eads, C. A., K. D. Danenberg, K. Kawakami, L. B. Saltz, C. Blake, D. Shibata, P. V. Danenberg, and P. W. Laird.** 2000. MethyLight: a high-throughput assay to measure DNA methylation. Nucleic Acids Res. **28:**E32.
17. **Eads, C. A., K. D. Danenberg, K. Kawakami, L. B. Saltz, P. V. Danenberg, and P. W. Laird.** 1999. CpG island hypermethylation in human colorectal tumors is not associated with DNA methyltransferase overexpression. Cancer Res. **59:**2302–2306.
18. **Eads, C. A., R. V. Lord, S. K. Kurumboor, K. Wickramasinghe, M. L. Skinner, T. I. Long, J. H. Peters, T. R. DeMeester, K. D. Danenberg, P. V. Danenberg, P. W. Laird, and K. A. Skinner.** 2000. Fields of aberrant CpG island hypermethylation in Barrett's esophagus and associated adenocarcinoma. Cancer Res. **60:**5021–5026.
19. **Eads, C. A., R. V. Lord, K. Wickramasinghe, T. I. Long, S. K. Kurumboor, L. Bernstein, J. H. Peters, S. R. DeMeester, T. R. DeMeester, K. A. Skinner, and P. W. Laird.** 2001. Epigenetic patterns in the progression of esophageal adenocarcinoma. Cancer Res. **61:**3410–3418.
20. **Edelmann, W., P. E. Cohen, M. Kane, K. Lau, B. Morrow, S. Bennett, A. Umar, T. Kunkel, G. Cattoretti, R. Chaganti, J. W. Pollard, R. D. Kolodner, and R. Kucherlapati.** 1996. Meiotic pachytene arrest in MLH1-deficient mice. Cell **85:**1125–1134.
21. **Edelmann, W., P. E. Cohen, B. Kneitz, N. Winand, M. Lia, J. Heyer, R. Kolodner, J. W. Pollard, and R. Kucherlapati.** 1999. Mammalian MutS homologue 5 is required for chromosome pairing in meiosis. Nat. Genet. **21:**123–127.
22. **Edelmann, W., K. Yang, M. Kuraguchi, J. Heyer, M. Lia, B. Kneitz, K. Fan, A. M. Brown, M. Lipkin, and R. Kucherlapati.** 1999. Tumorigenesis in Mlh1 and Mlh1/Apc1638N mutant mice. Cancer Res. **59:**1301–1307.
23. **Edelmann, W., K. Yang, A. Umar, J. Heyer, K. Lau, K. Fan, W. Liedtke, P. E. Cohen, M. F. Kane, J. R. Lipford, N. Yu, G. F. Crouse, J. W. Pollard, T. Kunkel, M. Lipkin, R. Kolodner, and R. Kucherlapati.** 1997. Mutation in the mismatch repair gene Msh6 causes cancer susceptibility. Cell **91:**467–477.
24. **El-Deiry, W. S., B. D. Nelkin, P. Celano, R. W. Yen, J. P. Falco, S. R. Hamilton, and S. B. Baylin.** 1991. High expression of the DNA methyltransferase gene characterizes human neoplastic cells and progression stages of colon cancer. Proc. Natl. Acad. Sci. USA **88:**3470–3474.
25. **Feinberg, A. P., C. W. Gehrke, K. C. Kuo, and M. Ehrlich.** 1988. Reduced genomic 5-methylcytosine content in human colonic neoplasia. Cancer Res. **48:**1159–1161.
26. **Fuks, F., W. A. Burgers, A. Brehm, L. Hughes-Davies, and T. Kouzarides.** 2000. DNA methyltransferase Dnmt1 associates with histone deacetylase activity. Nat. Genet. **24:**88–91.
27. **Goelz, S. E., B. Vogelstein, S. R. Hamilton, and A. P. Feinberg.** 1985. Hypomethylation of DNA from benign and malignant human colon neoplasms. Science **228:**187–190.
28. **Hansen, R. S., C. Wijmenga, P. Luo, A. M. Stanek, T. K. Canfield, C. M. Weemaes, and S. M. Gartler.** 1999. The DNMT3B DNA methyltransferase gene is mutated in the ICF immunodeficiency syndrome. Proc. Natl. Acad. Sci. USA **96:**14412–14417.
29. **Hare, J. T., and J. H. Taylor.** 1985. One role for DNA methylation in vertebrate cells is strand discrimination in mismatch repair. Proc. Natl. Acad. Sci. USA **82:**7350–7354.
30. **Hata, K., and Y. Sakaki.** 1997. Identification of critical CpG sites for repression of L1 transcription by DNA methylation. Gene **189:**227–234.
31. **Hellmann-Blumberg, U., M. F. Hintz, J. M. Gatewood, and C. W. Schmid.** 1993. Developmental differences in methylation of human Alu repeats. Mol. Cell. Biol. **13:**4523–4530.
32. **Herman, J. G., and S. B. Baylin.** 2000. Promoter-region hypermethylation and gene silencing in human cancer. Curr. Top. Microbiol. Immunol. **249:**35–54.
33. **Herman, J. G., A. Umar, K. Polyak, J. R. Graff, N. Ahuja, J. P. Issa, S. Markowitz, J. K. Willson, S. R. Hamilton, K. W. Kinzler, M. F. Kane, R. D. Kolodner, B. Vogelstein, T. A. Kunkel, and S. B. Baylin.** 1998. Incidence and functional consequences of hMLH1 promoter hypermethylation in colorectal carcinoma. Proc. Natl. Acad. Sci. USA **95:**6870–6875.
34. **Howell, C. Y., T. H. Bestor, F. Ding, K. E. Latham, C. Mertineit, J. M. Trasler, and J. R. Chaillet.** 2001. Genomic imprinting disrupted by a maternal effect mutation in the Dnmt1 gene. Cell **104:**829–838.
35. **Issa, J. P., P. M. Vertino, J. Wu, S. Sazawal, P. Celano, B. D. Nelkin, S. R. Hamilton, and S. B. Baylin.** 1993. Increased cytosine DNA-methyltransferase activity during colon cancer progression. J. Natl. Cancer Inst. **85:**1235–1240.
36. **Jackson-Grusby, L., C. Beard, R. Possemato, M. Tudor, D. Fambrough, G. Csankovszki, J. Dausman, P. Lee, C. Wilson, E. Lander, and R. Jaenisch.** 2001. Loss of genomic methylation causes p53-dependent apoptosis and epigenetic deregulation. Nat. Genet. **27:**31–39.
37. **Jackson-Grusby, L., P. W. Laird, S. N. Magge, B. J. Moeller, and R. Jaenisch.** 1997. Mutagenicity of 5-aza-2′-deoxycytidine is mediated by the mammalian DNA methyltransferase. Proc. Natl. Acad. Sci. USA **94:**4681–4685.
38. **Jones, P. A., and P. W. Laird.** 1999. Cancer epigenetics comes of age. Nat. Genet. **21:**163–167.
39. **Jones, P. L., G. J. Veenstra, P. A. Wade, D. Vermaak, S. U. Kass, N. Landsberger, J. Strouboulis, and A. P. Wolffe.** 1998. Methylated DNA and MeCP2 recruit histone deacetylase to repress transcription. Nat. Genet. **19:**187–191.
40. **Kautiainen, T. L., and P. A. Jones.** 1986. DNA methyltransferase levels in tumorigenic and nontumorigenic cells in culture. J. Biol. Chem. **261:**1594–1598.
41. **Knox, J. D., F. D. Araujo, P. Bigey, A. D. Slack, G. B. Price, M. Zannis-Hadjopoulos, and M. Szyf.** 2000. Inhibition of DNA methyltransferase inhibits DNA replication. J. Biol. Chem. **275:**17986–17990.
42. **Kochanek, S., D. Renz, and W. Doerfler.** 1995. Transcriptional silencing of human Alu sequences and inhibition of protein binding in the box B regulatory elements by 5′-CG-3′ methylation. FEBS Lett. **360:**115–120.
43. **Labow, M. A.** 1995. Use of lac activator proteins for regulated expression of oncogenes. Methods Enzymol. **254:**375–387.
44. **Labow, M. A., S. B. Baim, T. Shenk, and A. J. Levine.** 1990. Conversion of the lac repressor into an allosterically regulated transcriptional activator for mammalian cells. Mol. Cell. Biol. **10:**3343–3356.
45. **Laird, P. W.** 2000. Mouse models in DNA-methylation research. Curr. Top. Microbiol. Immunol. **249:**119–134.
46. **Laird, P. W., L. Jackson-Grusby, A. Fazeli, S. L. Dickinson, W. E. Jung, E. Li, R. A. Weinberg, and R. Jaenisch.** 1995. Suppression of intestinal neoplasia by DNA hypomethylation. Cell **81:**197–205.
47. **Laird, P. W., A. Zijderveld, K. Linders, M. A. Rudnicki, R. Jaenisch, and A.**

Berns. 1991. Simplified mammalian DNA isolation procedure. Nucleic Acids Res. **19:**4293.
48. **Lee, P. J., L. L. Washer, D. J. Law, C. R. Boland, I. L. Horon, and A. P. Feinberg.** 1996. Limited up-regulation of DNA methyltransferase in human colon cancer reflecting increased cell proliferation. Proc. Natl. Acad. Sci. USA **93:**10366–10370.
49. **Lei, H., S. P. Oh, M. Okano, R. Juttermann, K. A. Goss, R. Jaenisch, and E. Li.** 1996. De novo DNA cytosine methyltransferase activities in mouse embryonic stem cells. Development **122:**3195–3205.
50. **Lengauer, C., K. W. Kinzler, and B. Vogelstein.** 1997. DNA methylation and genetic instability in colorectal cancer cells. Proc. Natl. Acad. Sci. USA **94:**2545–2550.
51. **Leonhardt, H., A. W. Page, H. U. Weier, and T. H. Bestor.** 1992. A targeting sequence directs DNA methyltransferase to sites of DNA replication in mammalian nuclei. Cell **71:**865–873.
52. **Li, E., T. H. Bestor, and R. Jaenisch.** 1992. Targeted mutation of the DNA methyltransferase gene results in embryonic lethality. Cell **69:**915–926.
53. **Liu, W. M., and C. W. Schmid.** 1993. Proposed roles for DNA methylation in Alu transcriptional repression and mutational inactivation. Nucleic Acids Res. **21:**1351–1359.
54. **Lu, A. L., S. Clark, and P. Modrich.** 1983. Methyl-directed repair of DNA base-pair mismatches in vitro. Proc. Natl. Acad. Sci. USA **80:**4639–4643.
55. **MacLeod, A. R., and M. Szyf.** 1995. Expression of antisense to DNA methyltransferase mRNA induces DNA demethylation and inhibits tumorigenesis. J. Biol. Chem. **270:**8037–8043.
56. **Nakagawa, H., R. B. Chadwick, P. Peltomaki, C. Plass, Y. Nakamura, and A. de La Chapelle.** 2000. Loss of imprinting of the insulin-like growth factor II gene occurs by biallelic methylation in a core region of H19-associated CTCF-binding sites in colorectal cancer. Proc. Natl. Acad. Sci. USA **19:**19.
57. **Nan, X., F. J. Campoy, and A. Bird.** 1997. MeCP2 is a transcriptional repressor with abundant binding sites in genomic chromatin. Cell **88:**471–481.
58. **Nan, X., H. H. Ng, C. A. Johnson, C. D. Laherty, B. M. Turner, R. N. Eisenman, and A. Bird.** 1998. Transcriptional repression by the methyl-CpG-binding protein MeCP2 involves a histone deacetylase complex. Nature **393:**386–389.
59. **Ng, H. H., and A. Bird.** 1999. DNA methylation and chromatin modification. Curr. Opin. Genet. Dev. **9:**158–163.
60. **Okano, M., D. W. Bell, D. A. Haber, and E. Li.** 1999. DNA methyltransferases Dnmt3a and Dnmt3b are essential for de novo methylation and mammalian development. Cell **99:**247–257.
61. **Okano, M., S. Xie, and E. Li.** 1998. Cloning and characterization of a family of novel mammalian DNA (cytosine-5) methyltransferases. Nat. Genet. **19:** 219–220.
62. **Olek, A., J. Oswald, and J. Walter.** 1996. A modified and improved method for bisulphite based cytosine methylation analysis. Nucleic Acids Res. **24:** 5064–5066.
63. **Pao, M. M., G. Liang, Y. C. Tsai, Z. Xiong, P. W. Laird, and P. A. Jones.** 2000. DNA methylator and mismatch repair phenotypes are not mutually exclusive in colorectal cancer cell lines. Oncogene **19:**943–952.
64. **Prolla, T. A., S. M. Baker, A. C. Harris, J. L. Tsao, X. Yao, C. E. Bronner, B. Zheng, M. Gordon, J. Reneker, N. Arnheim, D. Shibata, A. Bradley, and R. M. Liskay.** 1998. Tumour susceptibility and spontaneous mutation in mice deficient in Mlh1, Pms1 and Pms2 DNA mismatch repair. Nat. Genet. **18:**276–279.
65. **Ramchandani, S., A. R. MacLeod, M. Pinard, E. von Hofe, and M. Szyf.** 1997. Inhibition of tumorigenesis by a cytosine-DNA, methyltransferase, antisense oligodeoxynucleotide. Proc. Natl. Acad. Sci. USA **94:**684–689.
66. **Reitmair, A. H., R. Schmits, A. Ewel, B. Bapat, M. Redston, A. Mitri, P. Waterhouse, H. W. Mittrucker, A. Wakeham, B. Liu, et al.** 1995. MSH2 deficient mice are viable and susceptible to lymphoid tumours. Nat. Genet. **11:**64–70.
67. **Robertson, K. D., S. Ait-Si-Ali, T. Yokochi, P. A. Wade, P. L. Jones, and A. P. Wolffe.** 2000. DNMT1 forms a complex with Rb, E2F1 and HDAC1 and represses transcription from E2F-responsive promoters. Nat. Genet. **25:**338–342.
68. **Robertson, K. D., and P. A. Jones.** 1997. Dynamic interrelationships between DNA replication, methylation, and repair. Am. J. Hum. Genet. **61:**1220–1224.
69. **Robertson, K. D., K. Keyomarsi, F. A. Gonzales, M. Velicescu, and P. A. Jones.** 2000. Differential mRNA expression of the human DNA methyltransferases (DNMTs) 1, 3a and 3b during the G(0)/G(1) to S phase transition in normal and tumor cells. Nucleic Acids Res. **28:**2108–2113.
70. **Robertson, K. D., E. Uzvolgyi, G. Liang, C. Talmadge, J. Sumegi, F. A. Gonzales, and P. A. Jones.** 1999. The human DNA methyltransferases (DNMTs) 1, 3a and 3b: coordinate mRNA expression in normal tissues and overexpression in tumors. Nucleic Acids Res. **27:**2291–2298.
71. **Robertson, K. D., and A. P. Wolffe.** 2000. DNA methylation in health and disease. Nat. Rev. Genet. **1:**11.
72. **Rountree, M. R., K. E. Bachman, and S. B. Baylin.** 2000. DNMT1 binds HDAC2 and a new co-repressor, DMAP1, to form a complex at replication foci. Nat. Genet. **25:**269–277.
73. **Sollbach, A. E., and G. E. Wu.** 1995. Inversions produced during V(D)J rearrangement at IgH, the immunoglobulin heavy-chain locus. Mol. Cell. Biol. **15:**671–681.
74. **Strand, M., T. A. Prolla, R. M. Liskay, and T. D. Petes.** 1993. Destabilization of tracts of simple repetitive DNA in yeast by mutations affecting DNA mismatch repair. Nature **365:**274–276.
75. **Toyota, M., N. Ahuja, M. Ohe-Toyota, J. G. Herman, S. B. Baylin, and J. P. Issa.** 1999. CpG island methylator phenotype in colorectal cancer. Proc. Natl. Acad. Sci. USA **96:**8681–8686.
76. **Tucker, K. L., C. Beard, J. Dausmann, L. Jackson-Grusby, P. W. Laird, H. Lei, E. Li, and R. Jaenisch.** 1996. Germ-line passage is required for establishment of methylation and expression patterns of imprinted but not of nonimprinted genes. Genes Dev. **10:**1008–1020.
77. **Umar, A., J. C. Boyer, and T. A. Kunkel.** 1994. DNA loop repair by human cell extracts. Science **266:**814–816.
78. **Umar, A., A. B. Buermeyer, J. A. Simon, D. C. Thomas, A. B. Clark, R. M. Liskay, and T. A. Kunkel.** 1996. Requirement for PCNA in DNA mismatch repair at a step preceding DNA resynthesis. Cell **87:**65–73.
79. **van Lohuizen, M., S. Verbeek, P. Krimpenfort, J. Domen, C. Saris, T. Radaszkiewicz, and A. Berns.** 1989. Predisposition to lymphomagenesis in pim-1 transgenic mice: cooperation with c-myc and N-myc in murine leukemia virus-induced tumors. Cell **56:**673–682.
80. **van Lohuizen, M., S. Verbeek, B. Scheijen, E. Wientjens, H. van der Gulden, and A. Berns.** 1991. Identification of cooperating oncogenes in E mu-myc transgenic mice by provirus tagging. Cell **65:**737–752.
81. **Veigl, M. L., L. Kasturi, J. Olechnowicz, A. H. Ma, J. D. Lutterbaugh, S. Periyasamy, G. M. Li, J. Drummond, P. L. Modrich, W. D. Sedwick, and S. D. Markowitz.** 1998. Biallelic inactivation of hMLH1 by epigenetic gene silencing, a novel mechanism causing human MSI cancers. Proc. Natl. Acad. Sci. USA **95:**8698–8702.
82. **Walsh, C. P., J. R. Chaillet, and T. H. Bestor.** 1998. Transcription of IAP endogenous retroviruses is constrained by cytosine methylation. Nat. Genet. **20:**116–117.
83. **Warbrick, E.** 1998. PCNA binding through a conserved motif. Bioessays **20:**195–199.
84. **Warbrick, E.** 2000. The puzzle of PCNA's many partners. Bioessays **22:**997–1006.
85. **Whitehurst, C. E., S. Chattopadhyay, and J. Chen.** 1999. Control of V(D)J recombinational accessibility of the D beta 1 gene segment at the TCR beta locus by a germline promoter. Immunity **10:**313–322.
86. **Xiong, Z., A. H. Wu, C. M. Bender, J. L. Tsao, C. Blake, D. Shibata, P. A. Jones, M. C. Yu, R. K. Ross, and P. W. Laird.** 2001. Mismatch repair deficiency and CpG island hypermethylation in sporadic colon adenocarcinomas. Cancer Epidemiol. Biomarkers Prev. **10:**799–803.
87. **Xu, G. L., T. H. Bestor, D. Bourc'his, C. L. Hsieh, N. Tommerup, M. Bugge, M. Hulten, X. Qu, J. J. Russo, and E. Viegas-Pequignot.** 1999. Chromosome instability and immunodeficiency syndrome caused by mutations in a DNA methyltransferase gene. Nature **402:**187–191.